Acta Crystallographica Section D
Biological Crystallography
ISSN 0907-4449

Structure of the neurotoxic complex vipoxin at 1.4 Å resolution

Sankaran Banumathi,[a] Kanagalaghatta R. Rajashankar,[a]† Corinna Nötzel,[a] Boris Aleksiev,[b] Tej P. Singh,[c] Nicolay Genov[d] and Christian Betzel[a]*

[a]Institute of Medical Biochemistry and Molecular Biology, c/o DESY, Building 22a, Notkestrasse 85, 22603 Hamburg, Germany, [b]University of Chemical Technology and Metallurgy, Sofia, Bulgaria, [c]Department of Biophysics, All India Institute of Medical Sciences, 110029 New Delhi, India, and [d]Institute of Organic Chemistry, Bulgarian Academy of Sciences, Sofia 1113, Bulgaria

† Present address: Brookhaven National Laboratory, Building 725A-X9, Upton, NY 11973, USA.

Correspondence e-mail: betzel@unisgi1.desy.de

Received 9 April 2001
Accepted 13 August 2001

PDB Reference: vipoxin, 1jlt.

Vipoxin is a neurotoxic postsynaptic heterodimeric complex from the venom of *Vipera ammodytes meridionalis*, the most toxic snake in Europe. It consists of a basic and highly toxic phospholipase A_2 and an acidic non-toxic protein inhibitor. The two polypeptide chains have the same chain length and share 62% amino-acid identity. Vipoxin is a unique example of evolution of the catalytic and toxic phospholipase A_2 functions into inhibitory and non-toxic functions. The crystal structure of the complex has been determined by the molecular-replacement method and refined to 1.4 Å resolution to an *R* factor of 18.2%. The complex formation decreases the accessible surface area of the two subunits by ~1480 Å^2, which results in a reduction of toxicity and catalytic activity. The catalytic and substrate-binding sites of the vipoxin phospholipase A_2 are identical or similar to those of other group I/II enzymes. Two 2-methyl-2,4-pentanediol molecules are present in the hydrophobic channel close to the active site. The two subunits lack calcium ions. The negatively charged Asp49 of the phospholipase A_2, which participates in the Ca^{2+}-binding sites of other snake-venom phospholipase A_2s, is neutralized by the side chain of Lys69 from the inhibitor. Attempts have been made to identify the toxicity region and to explain the reduced catalytic activity and toxicity of the phospholipase A_2 subunit.

1. Introduction

The neurotoxin vipoxin is the main lethal component of the venom of *V. ammodytes meridionalis*, the most toxic snake in Europe. It is a complex between a basic strongly toxic phospholipase A_2 (PLA_2; phosphatide 2-acylhydrolase; E.C. 3.1.1.4) and an acidic, non-toxic and catalytically inactive protein inhibitor (Inh). The venoms of other snakes inhabiting southeast Europe, *V. ammodytes ammodytes* and *V. ammodytes montandoni*, which are evolutionarily older, contain monomeric PLA_2s. The two components of vipoxin are highly homologous proteins with 62% sequence identity (Mancheva *et al.*, 1987). This is the first known example of such a high degree of structural homology between an enzyme and its natural protein inhibitor. Vipoxin PLA_2 is a group II A enzyme containing 122 amino-acid residues and seven disulfide bridges. It is a very unstable protein and loses its toxicity and catalytic activity irreversibly in a few days after separation from the complex even when stored at 273 K in a lyophilized form. In contrast, the neurotoxic complex is stable for more than 4 y (Aleksiev & Tchorbanov, 1976). Most probably, Inh evolved from PLA_2 and when associated with the enzyme reduces both the catalytic activity and toxicity. In this respect, vipoxin is the first reported example of transformation of enzymatic and toxic functions into inhibitory and

Table 1
Data-collection and refinement statistics.

Values in parentheses are for the last resolution shell (1.39–1.3 Å).

Space group	$P2_12_12_1$
Unit-cell parameters (Å)	a = 44.05, b = 54.71, c = 104.76
Crystal volume per dalton (V_M) (Å^3 Da^{-1})	2.32
Wavelength used (Å)	0.908
Data collection and refinement	
Resolution (Å)	20–1.37
No. of unique reflections	50300
R_{merge} (%)	6.7 (25.7)
Completeness (%)	99.1 (96.1)
Refinement statistics	
R value/R_{free} (%)	18.2/19.5
No. of amino acids	244
No. of solvent molecules	320 water and 2 MPD molecules
Average B factors (Å^2)	
Protein	15.7
Water molecule	42.4
MPD molecule	28.3
R.m.s. deviations from ideal values	
Bond distances (Å)	0.009
Bond angle (°)	1.47
Torsion angles (°)	22.8
Ramachandran plot: non-Gly residues in	
Most favoured regions (%)	89.9 (Inh), 91.5 (PLA_2)
Additionally allowed regions (%)	8.3 (Inh), 8.5 (PLA_2)
Generously allowed regions (%)	1.8 (Inh), 0 (PLA_2)
Disallowed regions (%)	0
Luzzati coorinate error (Å)	0.15
σ_A coordinate error (Å)	0.08

non-toxic functions. The neurotoxic complex also demonstrates a modulation of the toxic phospholipase function generated by molecular evolution. Comparison with other multichain neurotoxins showed that vipoxin is unique in many properties and differs from them in several pharmacological functions. The oligomeric toxins containing an active PLA_2 component are usually β-neurotoxins which bind to the neuronal presynaptic plasma membranes and affect neurotransmitter release (Bon, 1997). Vipoxin is an exception to this rule and is one of the few known multichain neurotoxins with postsynaptic toxicity (Tchorbanov *et al.*, 1978). It is an α-neurotoxin which acts on the postsynaptic membranes, preventing the binding of acetylcholine to its receptor and blocking the neuromuscular transmission of skeletal muscles. In this way the toxin exerts its lethal action. Another postsynaptic multimeric snake-venom toxin is α-bungarotoxin from the venom of *Bungarus multicinctus* (Gubensek *et al.*, 1997). β-Bungarotoxin is a presynaptic neurotoxin which acts on the presynaptic site or nerve site of the neuromuscular junctions (Bon, 1997). In contrast to the vipoxin PLA_2 and Inh, which are associated through non-covalent interactions, in β-bungarotoxin the PLA_2 subunit is covalently linked by a disulfide bridge to the second component of the neurotoxic complex, the so-called 'Kunitz' subunit (Bon, 1997). The presynaptic oligomeric crotoxin also differs from vipoxin in structure and pharmacological properties. Thus, the non-enzymatic component of vipoxin is monomeric, while the respective component of the crotoxin complex consists of three polypeptide chains (Breithaupt *et al.*, 1974). When isolated from the complex, the vipoxin PLA_2 manifests a presynaptic action (Tchorbanov *et al.*, 1978). Evidently, the complex formation changes the target of the pharmacological action of the neurotoxin and vipoxin is 'targeted' to the postsynaptic site.

The additional units in the PLA_2 multimeric complexes act like chaperones and help in specific binding of the enzyme to the target. Usually, they enhance the lethal potency of the PLA_2 subunit, as has been observed in the cases of neurotoxic complexes from *V. russelli formosensis* (Wang *et al.*, 1992), *V. aspis zinnikeri* (Komori *et al.*, 1996) and *Crotalus durissus* (Rübsamen *et al.*, 1971). However, in vipoxin Inh considerably reduces the lethal action of the PLA_2 component: a fivefold increase of the vipoxin PLA_2 toxicity was observed after separation from the inhibitor (Aleksiev & Tchorbanov, 1976). Recently, crystallization and preliminary X-ray diffraction studies on the toxin from *V. russelli formosensis* have been published (Rajashankar, Tsai *et al.*, 1999).

Here, we report the structure of the neurotoxic complex vipoxin refined to 1.4 Å resolution. A preliminary report on vipoxin structure in a different crystal form to 2.0 Å resolution has been previously reported (Perbandt *et al.*, 1997). To the best of our knowledge, this is the only known structure of a postsynaptic heterodimeric snake-venom neurotoxin whose PLA_2 subunit is a group II enzyme. Also, this is the first structure of a complex between a higly homologous enzyme and a natural protein inhibitor which has evolved from the enzyme and acquired an inhibitory function.

2. Materials and methods

Crude venom was obtained from the toxic gland of *V. ammodites meridionalis*. Homogeneous vipoxin was isolated by ion-exchange chromatography as described by Tchorbanov & Aleksiev (1981). A new stable crystal form of vipoxin suitable for high-resolution X-ray intensity data collection was obtained after extensive screening. The crystals grew within two weeks by the hanging-drop vapour-diffusion technique from a solution with a protein concentration of 10 mg ml^{-1} containing 5%(v/v) polyethylene glycol 4000 (PEG 4000) and 18%(v/v) 2-methyl-2-4-pentanediol (MPD) as precipitant at 287 K. Preliminary data on crystallization and structure analysis to 2.0 Å, based on a different crystal form, have been published previously (Rajashankar, Genov *et al.*, 1999; Perbandt *et al.*, 1997). New diffraction data were collected at 100 K with synchrotron radiation at DESY Hamburg on a flash-frozen crystal with approximate dimensions of 0.3 × 0.3 × 0.2 mm on the synchrotron beamline BW7B using a MAR image-plate scanner. The images were processed using the *DENZO* program package (Otwinowski & Minor, 1996). The initial phase problem was solved by molecular-replacement techniques applying the program *AMoRe* (Navaza, 1994) using the 2.0 Å model of vipoxin. The refinement was performed by molecular-dynamic techniques using the program *CNS* (Brunger *et al.*, 1998). The *CCP*4 program suite (Collaborative Computational Project, Number 4, 1994) and the program *TURBO-FRODO* (Roussel & Cambillau, 1991) were used for calculations and model building, respectively. The solvent molecules were added

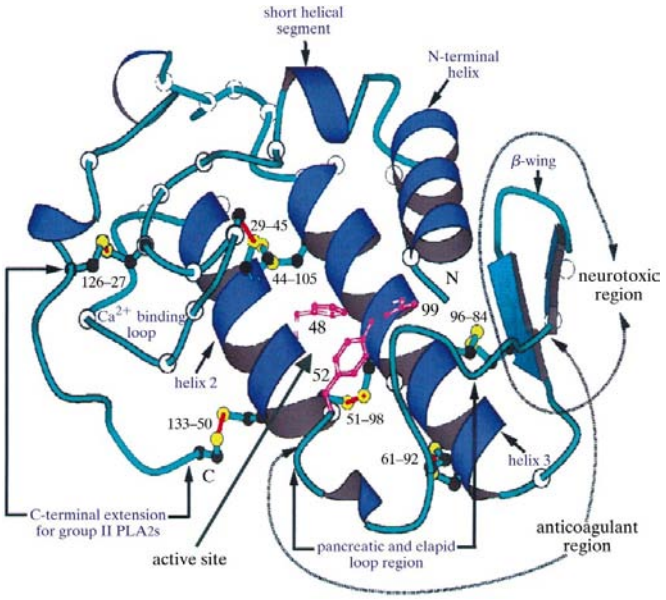

Figure 1
Ribbon representation of the PLA_2. The disulfide bridges and active-site residues are shown as ball-and-stick models. Secondary-structure regions and the Ca^{2+}-binding region as well as regions of pharmacological functions are labelled. Additionally, conserved and invariant residues found in approximately 200 sequences of PLA_2s (Danse *et al.*, 1997) are labelled at their C^{α} position.

subsequently during refinement at chemically reasonable positions where $(F_o - F_c)$ difference density exceeded 3σ. Ca^{2+} could not be identified, but two MPD molecules were clearly located in the hydrophobic channel. The final model of vipoxin contains 1911 non-H protein atoms, 320 water molecules and two MPD molecules. The occupancy for the atom C5 of one MPD molecule was defined to be 0.0, since the density at this region did not appear clearly. The crystallographic R and $R_{\rm free}$ factors were 18.2 and 19.5%, respectively, for the resolution range 20–1.4 Å. The final model has been analysed using the program *PROCHECK* (Laskowski *et al.*, 1993), which indicates that 90.7% of all residues fall into the most favoured region of the φ,ψ plane. The average isotropic B factor for all atoms of vipoxin is 16 $Å^2$. The electron density of all atoms of the model is well defined except for residues Lys86, Asn89 and Lys115 of the PLA_2, which are at the surface of the molecule. For these residues, electron densities are only visible up to the C^{β} atoms. Weak densities were also observed for residues Arg35 and Lys115 of the Inh, which are also at the surface of the molecule. The final stereochemical parameters and a summary of data-collection and refinement parameters are summarized in Table 1. The surface accessibility was calculated using the program *DSSP* (Kabsch & Sander, 1983).

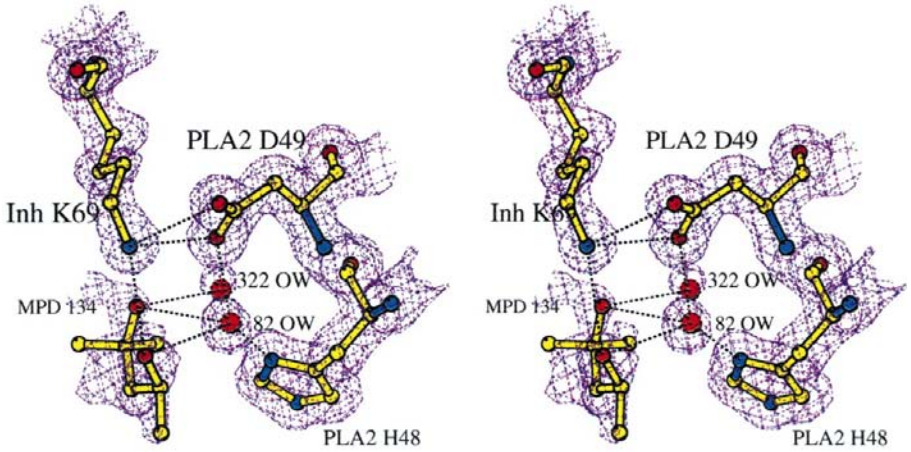

Figure 2
Stereo figure showing the electron density in the active-site region with superimposed amino acids, solvent water and one MPD molecule. All hydrogen bonds and interactions are indicated with their distances.

3. Results and discussion

3.1. Overall structure and dimeric organization of the neurotoxic complex

The vipoxin heterodimer is composed of two subunits with essentially identical folding. The whole complex has a close to globular shape and has dimensions of 30 × 55 × 32 Å. Each monomer has dimensions of approximately 12 × 40 × 25 Å. The overall structures of the subunits are similar to those of other snake-venom PLA_2s, as shown in Fig. 1. The secondary structure consists of three helices, two short helical segments and one section of antiparallel β-sheet. Two long and antiparallel α-helices include residues 40–54 and 89–109,

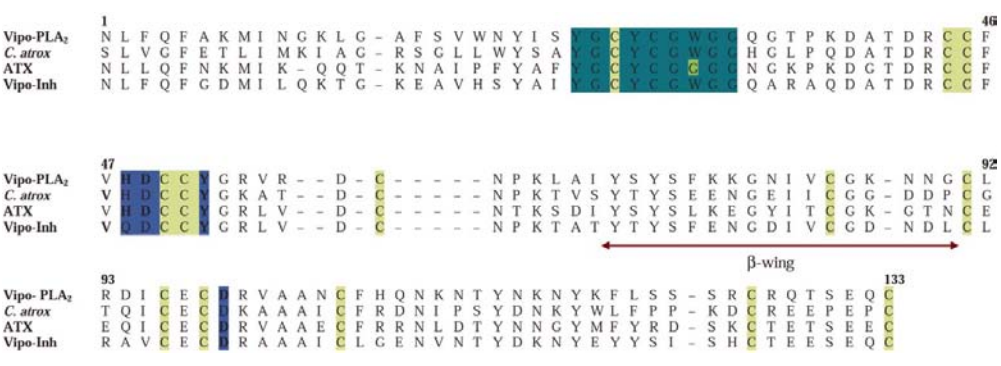

Figure 3
Amino-acid sequence comparison between vipoxin, *C. atrox* and *A. halys pallas* (agkistrodotoxin, ATX) PLA_2s and vipoxin inhibitor. The sequence identity between the vipoxin PLA_2 and the *C. atrox* and *A. halys pallas* PLA_2 is 48 and 59%, respectively. The sequence numbering is in accordance with that proposed by Renetseder *et al.* (1985). Blue columns indicate functional residues of the catalytic site and the residues involved in potential calcium binding are shown in green. The region of the β-wing is indicated accordingly and cysteines are shown in yellow.

Table 2
Hydrogen-bond contacts.

(*a*) Hydrogen-bond contacts of the MPD molecules (Å).

MPD134 O2	Inh Lys69 NZ	2.93
	OW323	2.46
	PLA_2 Asp49 OD1	3.25
	OW82	3.11
	OW322	2.85
	PLA_2 Gly30 N	2.68
	OW82	2.91
MPD135 O4	PLA_2 Trp31 NE1	2.72
	OW152	2.22

(*b*) Intermolecular hydrogen-bond contacts stabilizing the vipoxin complex.

PLA_2	Inh	Distance (Å)
Asn1 ND2	Gln34 OE1	2.97
Asn1 ND2	Gly33 O	3.20
Phe3 N	Gly32 O	2.91
Tyr28 O	Lys69 NZ	2.72
Gly30 O	Lys69 NZ	3.06
Gly32 O	Leu2 N	2.99
Gln34 OE1	Asn1 ND2	2.89
Asp49 OD2	Lys69 NZ	3.01
Asp49 OD1	Lys69 NZ	3.03
Asp49 O	Asn61 ND2	2.89
Asn61 ND2	Asp49 O	2.94
Lys69 NZ	Tyr28 O	2.83
Lys69 NZ	Asp49 OD1	2.64

(*c*) Internal solvent water hydrogen-bond contacts.

Solvent water	Inh	Distance (Å)
OW 1	Pro68 O	2.83
	Asp99 OD2	2.68
OW56	Tyr52 OH	2.73
OW122	Asn61 ND2	2.81
OW152	Trp31 NE1	2.95
OW318	Gln48 OE1	2.93
	Cys45 O	3.16
	Asp49 OD1	3.22
OW323	Lys69 NZ	3.12

Solvent water	PLA_2	Distance (Å)
OW82	Cys45 O	2.93
	His48 ND1	2.91
	Asp49 OD1	2.62
OW122	Asp49 OD1	3.09
OW152	Ile23 O	2.98
OW287	Tyr52 O	2.99
OW323	Gly30 O	3.06
OW322	His48 ND1	2.60
	Asp49 OD1	2.57
OW324	Lys69 NZ	3.06

respectively. They are connected with two disulfide bridges stabilizing this substructure. The third α-helix includes the N-terminal part of the polypeptide chain (residues 2–14). Leu2, Phe5, Met8 and Ile9 from this helix, which are conserved in both PLA_2 and Inh, participate in the formation of a hydrophobic channel leading to the catalytic site. During catalysis, the channel is occupied by the substrate. Approximately 50% of the residues of PLA_2 and Inh are included in α-helix structures. A loop of double-stranded antiparallel β-sheet is observed in the two components of the heterodimer. It includes residues 74–85 and extends outwards from the protein globule. This specific substructure is the only segment of β-sheet structure; it includes 15% of the residues and is defined as a 'β-wing'. It is conserved in group I/II/III PLA_2s (Scott, 1997). The 'β-wing' structure is more flexible and only partially stabilized by interaction with side chains of helix V. The tertiary structure is further stabilized by seven disulfide bridges, as shown in Fig. 1, which are typical of the group II secretory PLA_2s.

3.2. Active site, hydrophobic channel and Ca^{2+}-binding site

The catalytic residues of the vipoxin PLA_2 are shown with the superimposed electron density in Fig. 2. They include His48, Asp99 and a water molecule (OW82) which serves as a nucleophile during the catalysis. The X-ray model revealed the presence of the so-called 'catalytic network', a system of hydrogen bonds which involves the catalytic triad and additional two tyrosines, Tyr52 and Tyr73. Furthermore, the salt-bridge interaction between the PLA_2 and Inh subunit *via* Asp49 and Lys69 (Fig. 2) is particularly interesting. This specific hydrogen-bonding network stabilizes the region of the catalytic site and the conformation of the whole molecule. The arrangement of this site is, in principle, similar to that of other PLA_2s. It occupies a hydrophobic cavity which is opened toward the protein surface and connected with a hydrophobic channel. The hydrophobicity of this region is supported by the presence of two MPD (2-methyl-2,4-pentanediol) molecules. This confirms that monodisperse hydrophobic molecules can enter the vicinity of the hydrophobic channel. As displayed in Fig. 2, one MPD molecule participates in several interactions with active-site residues (Table 2*a*). MPD was used in the crystallization buffer and it is therefore striking to find it in the position that would be occupied by the free fatty acid liberated after the hydrolysis of phospholipids (Van Deeman & Haas, 1963). Snake-venom PLA_2s bind the acyl portion of substrates to such channels (Scott, 1997). This substructure was identified in both the vipoxin PLA_2 and Inh, and consists of Leu2, Phe5, Met8, Ile9, Tyr22, Cys29, Cys45, Ala102, Ala103 and Phe106 (Leu106 in Inh). The hydrophobic channel of the inhibitor can not function productively because the non-toxic subunit lacks enzymatic activity. Vipoxin was crystallized in the absence of added calcium and for this reason the two subunits lack metal ions. In the secretory PLA_2s, the Ca^{2+}-binding loop includes residues 25–33. The metal ion is coordinated by O atoms of Asp49 (two carboxylate O atoms) and the carbonyl O atoms of Tyr28, Gly30 and Gly32 as well as two water molecules. This loop forms one of the walls of the hydrophobic channel and for this reason is important for the enzyme–substrate interactions. Calcium stabilizes the substructure mentioned above; in the absence of metal ion the loop is conformationally flexible. In vipoxin, the carbonyl O atoms of residues 28 and 32 from the PLA_2 subunit are involved in intermolecular contacts with the inhibitor (Table 2*b*) and the O atom of the CO group of residue 32 is 5.5 Å away from the potential calcium-binding site. However, the negative charge of the PLA_2 Asp49 is

Table 3
Charged residues at pH 6–7, not including the C and N termini, and aromatic residues of the vipoxin PLA_2 and Inh, in comparison to the PLA_2s from *C. atrox* (PDB entry 1pp2) and *A. halys pallas* (agkistrodotoxin, ATX; PDB entry 1a2a); SA: surface accessibility.

	PLA_2	Inh	*C. atrox*	ATX
Arg(+)	7	5	4	6
Asp(−)	5	10	10	7
Glu(−)	2	8	8	10
Lys(+)	9	4	6	9
Total	23	27	28	32
+ve	16	9	10	15
−ve	7	18	18	17
Salt bridges	7	7	7	7
Trp	2	1	3	0
Tyr	8	10	8	10
Phe	7	4	4	6
SA (Å^2)	7432	7115	7147	6965
SA (Å^2) dimer	11586		11787	12085

neutralized by the positively charged alkylammonium side chain of Lys69 from Inh and *vice versa*. This salt bridge, as shown in Fig. 2, stabilizes the region which in other secretory PLA_2s is occupied by a Ca^{2+} ion.

3.3. Inhibitor

Inh is a multifunctional subunit of the vipoxin complex and it appears that it evolved from the closely related PLA_2 by divergent evolution. The high degree of sequence homology (62%), the identical length of the polypeptide chains (122 residues) and the high three-dimensional structure similarity confirm this hypothesis. In the neurotoxic complex, Inh plays physiological as well as structural functions. The toxic PLA_2 preserves its pharmacological activity for a long time owing to the complex formation with the non-toxic component. Inh is catalytically inactive owing to the substitution of the active site His48 with Gln48 (Fig. 3). Inh stabilizes the unstable PLA_2 through ionic and hydrophobic interactions and in this way the toxic subunit of the complex preserves the catalytically and physiologically active conformation. All direct interactions are summarized in Table 2(*b*). Furthermore, 13 solvent water molecules are buried inside the PLA_2–Inh interface and provide an intensive hydrogen-bonding network, as summarized in Table 2(*c*), which further enhances the stabilization of the vipoxin complex. We have shown that the complex formation between PLA_2 and Inh increases the free energy of stabilization in water of vipoxin by 6–10 kJ mol^{-1} in comparison to that of the components (Genov *et al.*, 1998). The non-toxic inhibitor is an acidic protein with a pI of 4.6, while the strongly toxic PLA_2 is a basic subunit with a pI of 10.4 (Tchorbanov *et al.*, 1978). The drastic change in the charge (see also Table 3) may be responsible, at least in part, for the lack of toxicity. The predominant negative charge of Inh should create a repulsion of its molecule from the anionic

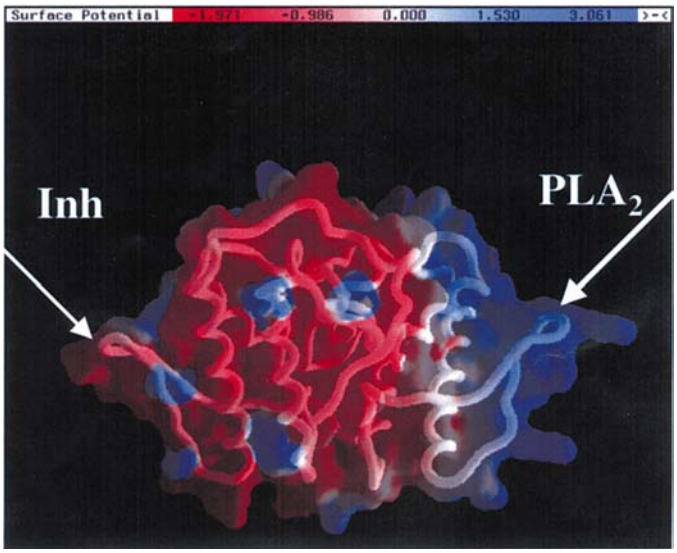

Figure 4
Surface potential, prepared using the program *GRASP* (Nicholls *et al.*, 1991), of the complex vipoxin with underlaid C^{α} worm. The active PLA_2 is on the right and the Inh on the left side. The arrows point towards the β-wing and the colour code is according to the surface potential, with values indicated by the crossbar. The electrostatic differences between the two protein chains are obvious, specifically in the region of the proposed toxic β-wing site.

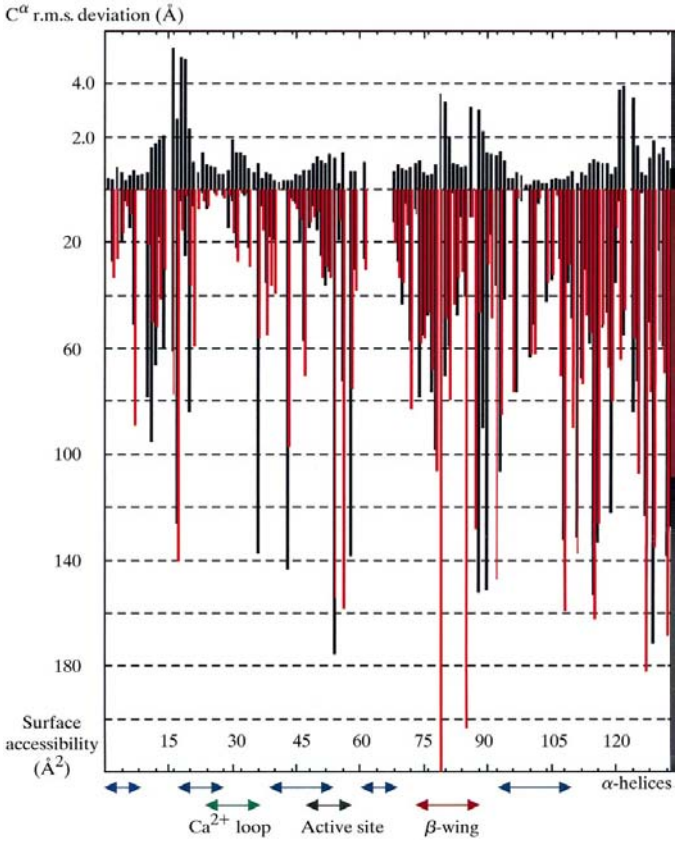

Figure 5
C^{α} r.m.s. plot between the vipoxin PLA_2 and inhibitor *versus* the surface accessibility. The surface accessibility was calculated for the individual uncomplexed molecules using the program *DSSP* (Kabsch & Sander, 1983). The blue bars represent the surface accessibility for the PLA_2 and the red bars that for the Inh. On the *x* axis the α-helices are indicated by blue arrows; the region of the Ca^{2+} loop, active site and β-wing are labelled accordingly.

membrane surface. Inh covers part of the enzyme–substrate binding site and this may explain the inhibitory effect of the non-toxic subunit. The entrance to the active site of PLA_2 is partially shielded by Inh and this makes the hydrolysis of substrate molecules difficult. However, the complex formation does not drastically disturb the access of small substrates to the PLA_2 active site as shown by the presence of MPD molecules: vipoxin is enzymatically active, although the activity is reduced. Vipoxin binds specifically to postsynaptic membranes, which means selective interaction with the target receptor. However, the PLA_2 separated from the complex shows presynaptic activity. Therefore, the binding of Inh to the enzyme seems to change the target of the physiological attack from the pre- to postsynaptic site of neuromuscular junctions. Consequently, it can be assumed that Inh is involved in the specific binding of the neurotoxin to the membrane as a 'chaperone' directing the PLA_2 subunit to its acceptor and preventing non-specific binding or participating in a transient complex Inh–PLA_2–acceptor. Such a synergism between enzymatic and non-enzymatic subunits has been described for crotoxin (Bon, 1997).

The inhibitory and neurotoxic components of vipoxin are highly homologous closely related proteins with very similar three-dimensional structures. One of them is a strongly toxic protein, while the other is completely devoid of toxicity. Comparison of the regions supposed to be responsible for the toxicity, mainly the β-wing and the segment including residues 115–128 (Wang *et al.*, 1992), showed drastic changes in the electrostatic charge, which can be seen in Fig. 4. The β-wing of PLA_2 contains positively charged residues, while the same loop of double-stranded antiparallel β-sheet in Inh is negatively charged. Also, the segment between residues 115–128 has a positive charge in PLA_2 and a negative charge in Inh. Most probably, the electrostatic charge is important for the presence or absence of toxicity in PLA_2 and Inh, respectively.

3.4. Comparison of PLA_2 and inhibitor

The C^{α} positions of the two polypeptide chains of PLA_2 and Inh were superimposed with an r.m.s. difference of 1.5 Å and a maximum displacement of 5.4 Å. Larger differences between the two monomers were observed in the flexible surface region including residues 16–20 between helix I and helix II at the N-terminus, residues 79–81 (the β-turn of the β-wing) and the C-terminal region 121–124, as shown in Figs. 5 and 6. Fig. 6 also shows the superposition of the C^{α} chain of the homologous PLA_2 from *C. atrox* (PDB entry 1pp2; Keith *et al.*, 1981), which resulted in an r.m.s. value of 1.6 Å and a maximal displacement of 4.7 Å. The vipoxin PLA_2 was finally superimposed on the PLA_2 of *Agkistrodron halys pallas* (PDB entry 1a2a; Tang *et al.*, 1998), with a corresponding r.m.s. value of 1.6 Å and a maximum displacement of 5.4 Å. All three neurotoxins belong to the group II PLA_2s and are closely related proteins with sequence homologies in the range 50–60% (Fig. 3). They all consist of 122 amino acids, have a dimer conformation and are structurally stabilized by seven salt bridges. The distribution of functionally important charged and aromatic residues is remarkably different (Table 3). Structural differences are found mainly in the C terminus and in the region of the β-wing, indicating the functional flexibility of this region. Finally, the C^{α} chain of vipoxin was superimposed on the 2.0 Å resolution structure (Perbandt *et al.*, 1997), resulting in an r.m.s. value of 0.8 Å and a maximum displacement of 4.4 Å.

The vipoxin X-ray model was inspected in order to find the structural basis of the recognition specificity of Inh for PLA_2. The complex is stabilized by hydrophobic, ionic and hydrogen-bond interactions. The intermolecular interactions stabilizing the neurotoxin are summarized in Table 2(*b*) and 2(*c*). The backbone carbonyl O atoms of Tyr28, Gly32, Val55 and Gly59 of PLA_2 are bonded to Lys69 N^{ζ}, Leu2 N and Asn56 $N^{\delta 2}$ from the inhibitor, respectively. Backbone carbonyl O atoms from the inhibitor are also bonded to side-chain atoms of the toxic subunit polypeptide chain. The complex is also stabilized by a salt bridge between the carboxylic O atoms of Asp49 from PLA_2 and Lys69 N^{ζ} of Inh. The interface between the two subunits can be considered as a 'recognition surface' for the specific binding of Inh to PLA_2. This interface includes two tryptophyl residues from the toxic subunit, Trp20 and Trp31, and one tryptophan, Trp31, from the non-toxic component of the complex. Hydrophobic interactions in which the bulky side chains of tryptophans are involved play an important role for the stabilization of protein complexes as well as in the interfacial binding (Sumandea *et al.*, 1999). The loss of accessible surface area upon the complex formation is 1480 $Å^2$. This represents 13% of the whole accessible surface area of vipoxin (Table 3). In addition to hydrophobic forces, electrostatic interactions between the two oppositely charged subunits, basic PLA_2 and acidic Inh, are important for the formation of the enzyme–inhibitor complex.

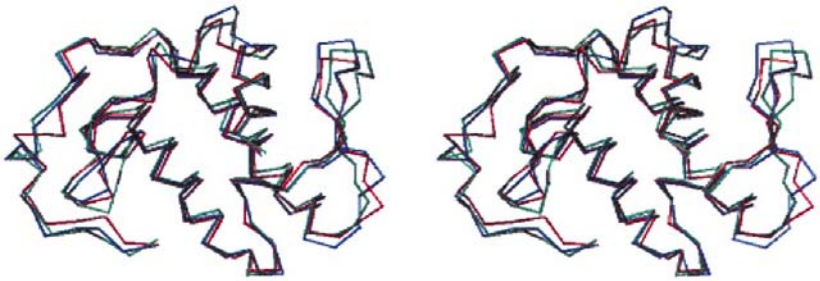

Figure 6
Stereoview of a C^{α} superposition of the neurotoxic vipoxin PLA_2 (blue), Inh (red) and *C. atrox* PLA_2 (yellow).

3.5. Interfacial adsorption surface

PLA_2 is an enzyme which catalyzes the hydrolysis of phospholipids at the lipid–water interface. The interfacial adsorption surface of snake-venom PLA_2s is located at the N-terminus of the polypeptide chain and includes residues surrounding the external opening of the hydrophobic channel: 1–3, 6–7,

10, 17–21, 23–24, 31, 67, 69–70, 72, 118–119, 121 and 124–125 (Heinrikson & Kezdy, 1990). It was shown that in addition to hydrophobic interactions, charged residues play an important role in optimizing interfacial catalysis (Han *et al.*, 1997). It appears that positively charged residues facilitate the penetratability of PLA_2; *i.e.* the insertion of the enzyme into the phospholipid membrane, which is important for the further hydrolysis of the membrane's phospholipids. There are four positively charged residues in the region of the interfacial recognition site of the vipoxin PLA_2, Lys7, Lys69, Lys118 and Arg125, which can play important role in the binding and orientation of the toxin at the membrane lipid–water interface. At the same time, there are no negatively charged residues in this site; *i.e.* the net electrostatic charge of the recognition surface is positive. On the contrary, there are three negatively charged residues in the same region of the non-toxic polypeptide chain and only one positively charged functional group. This means that the net electrostatic charge of the respective surface of Inh is negative, which should create electrostatic repulsion from anionic interfaces and correlates with the lack of toxicity of this subunit. Some of the substitutions in the recognition site of Inh, K7D, F17E, K118E and R125H, are radical and lead to a drastic change in the electrostatic charge of the region important for the formation of the complex with a membrane.

3.6. Neurotoxic site

The neurotoxic site(s) of PLA_2 ensures the binding of the neurotoxin to the target neuromembrane and the realisation of the pharmacological activity. These sites are separated from the catalytic site (Kini, 1997). However, some progress in the location of neurotoxic sites on the toxin molecule and in understanding the mechanism of their interactions with the respective receptors has been made (Krizaj *et al.*, 1989). The pharmacological effects of PLA_2 were investigated by *in vitro* methods and using isolated tissues, which sometimes led to non-specific effects. Nevertheless, successful experiments allowing the localization of the parts of the PLA_2 surface responsible for the toxicity have been reported. Thus, immunological investigations of the neurotoxin ammodytoxin A from *V. ammodytes ammodytes* revealed two sites of toxicity located in the C-terminal half of the molecule between residues 106–113 and 113–121 (Gubensek *et al.*, 1997). Residues 6, 12, 76–81 (β-wing) and 119–125 from the toxic component RV4 of the *V. russelli formosensis* dimeric toxin were identified as important for the toxicity (Wang *et al.*, 1992). The components of this neurotoxin show 92% sequence identity to the respective subunits of vipoxin and a high degree of homology was observed in the regions identified as sites of toxicity in RV4. The model of vipoxin shows that these regions are located on the protein surface and can interact with acceptors. Inh partially blocks the segment 119–125 of the toxic subunit. This can explain, at least in part, the reduced toxicity of PLA_2 when it is complexed with Inh. The region including the β-wing structure is largely exposed to the solvent and can interact with the respective membrane receptor.

4. Conclusions

The high-resolution crystal structure of the neurotoxin vipoxin provides detailed information about the nature of the forces crucial for the binding of the non-toxic protein inhibitor to the toxic and enzymatically active subunit. The complex formation is absolutely necessary for the preservation of the catalytic and pharmacological activities of the unstable PLA_2. Other important result of the binding of Inh to PLA_2 is the change in the target of physiological attack: the complex exhibits postsynaptic neurotoxicity, while the isolated enzyme is a presynaptic toxin. The high affinity of Inh for PLA_2 is a consequence of specific hydrophobic and electrostatic interactions between the 'recognition site' of the inhibitory subunit and the respective binding surface of the toxic polypeptide chain. Vipoxin is a unique example of modulation of the catalytic and toxic functions of a snake-venom PLA_2 generated by divergent evolution. In this respect, the three-dimensional model of the neurotoxin is of pharmacological interest and has provided new insights for structure-based drug-design studies.

The authors thank the Deutsche Forschungsgemeinschaft for financial support by the Project 436 BUL 113/115/01. These investigations were also supported by a grant from DAAD (Deutscher Akademischer Austauschdienst, Germany) and by a grant from the Department of Science and Technology (DST), New Delhi in terms of the Project Based Personnel Exchange.

References

Aleksiev, B. & Tchorbanov, B. (1976). *Toxicon*, **14**, 477–485.
Bon, C. (1997). *Venom Phospholipase A_2 Enzymes: Structure, Function and Mechanism*, edited by R. M. Kini, pp. 269–286. Chichester: John Wiley & Sons.
Breithaupt, H., Rübsamen, K. & Habermann, E. (1974). *Eur. J. Biochem.* **49**, 333–340.
Brunger, A. T., Adams, P. D., Clore, G. M., DeLano, W., Gros, P., Grosse-Kunstleve, R. W., Jiang, J. S., Kuszewski, J., Nilges, M., Pannu, N. S., Read, R. J., Rice, L. M., Simonson, T. & Warren, G. L. (1998). *Acta Cryst.* D**54**, 905–921.
Collaborative Computational Project, Number 4 (1994). *Acta Cryst.* D**50**, 760–763.
Danse, J. M., Gasparini, S. & Menez, A. (1997). *Venom Phospholipase A_2 Enzymes: Structure, Function and Mechanism*, edited by R. M. Kini, pp. 29–72. Chichester: John Wiley & Sons.
Genov, N., Dolashka, P., Aleksiev, B., Mancheva, I., Rajashankar, K. & Betzel, Ch. (1998). *Spectrochim. Acta A*, **54**, 1117–1125.
Gubensek, F., Krizai, I. & Pungercar, J. (1997). *Venom Phospholipase A_2 Enzymes: Structure, Function and Mechanism*, edited by R. M. Kini, pp. 245–268. Chichester: John Wiley & Sons.
Han, S. K., Yoon, E. T., Scott, D. L., Sigler, P. B. & Cho, W. (1997). *J. Biol. Chem.* **272**, 3573 -3582.
Heinrikson, R. L. & Kezdy, F. J. (1990). *Adv. Exp. Med. Biol.* **279**, 37–47.
Kabsch, W. & Sander, C. (1983). *Biopolymers*, **22**, 2577–2637.
Keith, C., Feldman, D. S., Deganello, S., Glick, J., Ward, K. B., Jones, E. O. & Sigler, P. B. (1981). *J. Biol. Chem.* **256**, 8602–8607.
Kini, R. M. (1997). Editor. *Venom Phospholipase A_2 Enzymes: Structure, Function and Mechanism*, pp. 1–28. Chichester: John Wiley & Sons.

Komori, Y., Masuda, K., Nikai, T. & Sugihara, H. (1996). *Arch Biochem. Biophys.* **327**, 303–307.
Krizaj, I., Turk, D., Ritonja, A. & Gubensek, F. (1989). *Biochim. Biophys. Acta*, **999**, 198–202.
Laskowski, R. A., MacArthur, M. W., Moss, D. S. & Thornton, J. M. (1993). *J. Appl. Cryst.* **26**, 283–91.
Mancheva, I., Kleinschmidt, T., Aleksiev, B. & Braunitzer, G. (1987). *Biol. Chem. Hoppe-Seyler*, **368**, 343–352.
Navaza, J. (1994). *Acta Cryst.* A**50**, 157–163.
Nicholls, A., Sharp, K. A. & Honig, B. (1991). *Proteins*, **11**, 281–296.
Otwinowski, Z. & Minor, W. (1996). *Methods Enzymol.* **276**, 307–326.
Perbandt, M., Wilson, J. C., Eschenburg, S., Mancheva, I., Aleksiev, B., Genov, N., Willingmann, P., Weber, W., Singh, T. P. & Betzel, Ch. (1997). *FEBS Lett.* **412**, 573–577.
Rajashankar, K. R., Genov, N., Alesksiev, B., Singh, T. P. & Betzel, Ch. (1999). *Perspectives in Structural Biology*, edited by M. Vijayan, N. Yathindra & A. S. Kolaskar, pp. 108–116. Hyderabad: University Press.
Rajashankar, K. R., Tsai, I. H. & Betzel, Ch. (1999). *Acta Cryst.* D**55**, 1064–1065.
Renetseder, R., Brunie, S., Dikstra, B. W., Drenth, J. & Siegler, P. B. (1985). *J. Biol. Chem.* **260**, 11627–11634.
Roussel, A. & Cambillau, C. (1991). *Silicon Graphics Geometry Partners Directory*, pp. 86–89. Mountain View, CA: Silicon Graphics.
Rübsamen, K., Breithaupt, H. & Habermann, E. (1971). *Naunyn-Schmiedebergs Arch. Exp. Pathol Pharmakol.* **270**, 274–280.
Scott, D. (1997). *Venom Phospholipase A_2 Enzymes: Structure, Function and Mechanism*, edited by R. M. Kini, pp. 97–128. Chichester: John Wiley & Sons.
Sumandea, M., Das S., Sumandea, C. & Cho, W. (1999). *Biochemistry*, **38**, 16290–16297.
Tang, L., Zhou, Y. C. & Lin, Z. J. (1998). *J. Mol. Biol.* **282**, 1–11.
Tchorbanov, B. & Aleksiev, B. (1981). *J. Appl. Biochem.* **3**, 558–561.
Tchorbanov, B., Grishin, E., Aleksiev, B. & Ovchinnikov, Y. (1978). *Toxicon*, **16**, 37–44.
Van Deeman, L. L. & Haas, G. H. (1963). *Biochem. Biophys. Acta*, **70**, 538–553.
Wang, Y.-M., Lu, P.-J., Ho, C.-L. & Tsai, I.-H. (1992). *Eur. J. Biochem.* **209**, 635–641.